On the Deep Western Boundary Current south of Cape Cod

Terrence M. Joyce
Jane Dunworth-Baker
Robert S. Pickart
Daniel Torres
Stephanie Waterman

Date: 4/30/2004
Submitted to: Deep-Sea Research II

Corresponding Author: Terrence M. Joyce
WHOI
360 Woods Hole Rd.
Woods Hole, MA 02543
tjoyce@whoi.edu

Abstract

Using CTD/oxygen data from eight cruises in the decade from 1994-2003, we have constructed a mean 'section' of properties across the Deep Western Boundary Current south of Cape Cod near 70°W. Since all sections included direct velocity measurements, our composite section enables us to portray the mean water mass structure as well as the flow field. Inshore of the Gulf Stream and between the 2500 and 4000m isobaths, the flow is to the southwest along the bathymetry and is remarkably barotropic. The equatorward flowing Labrador Sea Water is shown to have high dissolved oxygen, and low salinity and low potential vorticity, while the underlying Overflow Water is high in oxygen. Because the flow is largely barotropic, there is little vertical flow structure coincident with water mass changes associated with the deep high latitude source waters for the thermohaline circulation (THC), the North Atlantic Deep Water (NADW). Transport estimates for the cold limb of the THC give a range of –14 to –19 Sv. for the N. Atlantic source waters found on the section The greatest uncertainty is due to the presence of a Warm-Core Ring on one of the sections, which apparently completely reversed the flow in the DWBC. Offshore of the DWBC, some of the deep source waters are returned to the north in the deep Gulf Stream. The section is compared to two other, widely separated locations (Abaco and 55°W) which have markedly different characteristics of the DWBC.

1. **Introduction**

The flow and properties of the Deep Western Boundary Current (DWBC) change significantly during its transit through the N. Atlantic Ocean. At 55^{o}W, Pickart and Smethie (1998) show the core of maximum equatorward flow of Labrador Sea Water (LSW) and Iceland and Denmark Strait Overflow Water largely coincides with the tracer cores of salinity, potential vorticity (PV), and/or oxygen. We define PV to be $(-f/\rho_\theta)(\partial\rho_\theta/\partial z)$. Equatorward transports of these deep density classes were estimated (from 4 cruises) to be -18.9 ±6.3 Sv. and are mostly found over sloping bathymetry between 2000 and 4000m depth. In contrast, offshore of Abaco at 26.5^{o}N, Leaman and Harris (1990) found the deep southward flow over relatively flat topography with a much greater transport (-34.8 ±14.5 Sv.). In both cases, the error bars are based on the sample standard deviation, not the error of the 'mean'. In the Abaco section, the issue of deep recirculation was raised to explain the discrepancy between the measured transport and that estimated from tracer measurements (Fine and Molinari, 1988). Deep recirculation, as pointed out by Schmitz and McCartney (1993), could recycle much of the actual transport with smaller net throughflow of the deep water. In fact, the Pickart and Smethie estimates are not immune to effects of deep recirculation, although Hogg *et al.* (1986) place the northern recirculation gyre of the Gulf Stream in somewhat deeper water than the DWBC flow as noted by Pickart and Smethie (1998).

We study a third site between the above two, at 70^{o}W, before the DWBC crosses under the Gulf Stream. This site has been relatively well-measured with hydrographic cruises having direct velocity measurements, which we will see are essential to defining the deep transport. The cruises (Table 1) span a 10 year period from 1994 – 2003, and were taken mostly for other purposes than to estimate the transport and structure of the DWBC. However, the repeated measurement of tracers such as oxygen (and salinity), and direct velocity measurements with a Lowered Acoustic Doppler Current Profiler (LADCP) have provided an opportunity to construct a 'mean' section at this location as well. As this site will soon be instrumented for a four year period of deep transport measurements from moorings (http://www.whoi.edu/institutes/occi/currenttopics/ct_oms_stationw.html), this

summary represents what is known about the structure and transport of the DWBC prior to the array deployment. Indeed, a one year time series at a single point on the section constitutes one of our early moored "data points" for this report.

2. **Data discussion and mean property sections**

Station data from 8 cruises (Table 1) and from a one year deployment of a moored profiler mooring (Doherty et al., 1999) include CTD/LADCP stations taken at a number of sites over a period of years. The station velocity data have been obtained with a LADCP, and have been processed using standard methods (Fischer and Visbeck, 1993). Hydrographic data were collected with a Conductivity, Temperature, 'Depth', Oxygen ($CTDO_2$) instrument, with salinity and oxygen calibrated to water samples collected on a Rosette. We show the position of these stations (Figure 1), which define a "line" normal to the bathymetry, starting at the shelf break and extending seaward into the Sargasso Sea. A least square fit to a straight line determines the local distance and depth for each station relative to an origin (shown in Fig. 1). Since most stations were in shallow (<3000m) water, our ensemble for deeper depths is rather small, reducing to two cruises from 4000m out to 4500m water depth, and one cruise beyond that. Only two cruises were far enough offshore to encounter the Gulf Stream and only one (the last) was across it into the Sargasso Sea. Thus our ensemble will represent varying degrees of freedom as we construct mean property sections. Velocity data are decomposed into parallel and normal components to our section, and a filter with Gaussian half widths of 25 km (in the horizontal) and 50m (in the vertical) is used to define weights for gridding onto a regular distance, depth grid. Etop05 minute resolution bathymetry was linearly interpolated to determine local water depths and to define a depth/distance 'mask' for use with section plots and when estimating volume transports. The moored profiler, located at the 3000m isobath, was given an equivalent weight of 10 stations, as it represented a one year mean for the location.

From mean of the measured temperature and salinity, potential temperature, neutral density, and potential vorticity (ignoring relative vorticity) were then estimated. Density

levels appropriate to define the LSW and Overflow/Lower Deep Water (LDW) were then used to define boundaries for vertical integration of cross-stream velocity (transport), which will be presented in the next section. Here we discuss the mean property sections from our ensemble (Figs. 2,3).

The ensemble-average hydrographic structure as a function of distance offshore of the shelf break is given in Figs. 2 and 3. In the upper 500m, the potential temperature and salinity clearly show their most rapid changes upon entering the Gulf Stream (offshore distance of ca. 250 km). Within the Gulf Stream, large positive velocities are found with mean values above 80 cm/s. One can see from the sections that although Sargasso Sea Water is encountered at the far right of the section (note the salinity maximum and the thickening of the temperature contours associated with Eighteen Degree Water), still within the northward surface flow, and density surfaces continue to deepen in the offshore direction at the offshore extremity of the section.

The deeper levels of NADW are our main interest here, as they are involved with the transport of low salinity, high oxygen waters from the Labrador Sea, and high oxygen Overflow waters. At inshore depths along the continental slope, one can see evidence for more pristine versions of these water masses, with evidence for the water mass signal deepening offshore along density surfaces and slowly losing its signature as one crosses the deep Gulf Stream. The low PV signal associated with the convectively formed LSW stands out as a useful water mass signature as well.

As discussed by Pickart and Smethie (1993), the effect of Topographic Rossby Waves (TRWs), which have wavelengths of 100km and amplitudes of 5 cm/s, can cause substantial variability in the observed velocity in this region. Since several of our sections have a limited number of stations (Table 1), spatial filtering was not done prior to ensemble averaging individual current profiles. We have relied on enough members of the ensemble to remove the TRW influence. However, as the distribution of stations is not homogeneous, the TRW elimination is better closer to shore, where there are more stations. Since the TRWs are low mode, vertical averaging will not eliminate their

influence, whereas lateral averaging will. For our section-averaged transports, we estimate this transport 'error' to be of order 2 Sv. (1 Sv = 10^6 m^3/s) for the layer of NADW. We will later see that other factors can induce comparable uncertainty in layer transports.

On the inshore side of the Gulf Stream, the mean flow is in the opposite direction. It is much weaker than the Gulf Stream near the surface and more barotropic, with little *vertical* variation that can be linked with *vertical* changes in water masses through the deep layers flowing towards the equator, except perhaps for a slight increase in equatorward flow within the Overflow waters at 3500m depth. The equatorward flowing waters of LSW origin are clearly more "pristine" than the poleward flowing counterparts, having a better tracer signature, although one might argue that some LSW is actually moving to the north within the deep Gulf Stream. We will say more about this later as it is linked to deep recirculation. Most of the equatorward flow is found between the 2500 and 4000m isobaths. In the deepest levels at the offshore end of the section, there is a suggestion of increased equatorward flow again, but we hasten to point out that beyond the 4500m isobath, our ensemble amounts to only one occupation of the section! On the inshore side of the section inside of the 2500m isobath, flows are weak and for a small segment of the section, again positive, but with weak mean flows (1 cm/s) and no significant transport, as we shall soon see.

3. **Transports**

We have defined three layers by their neutral density (Table 2), and will focus mainly on the flow of the deeper two layers: one containing various types of LSW, and one containing Overflow Water as well as LDW, which is a mixture of Overflow and Antarctic Bottom Water. Volume transports of these layers (Fig. 4) are estimated as well as their cumulative transport starting at the shelf break origin. Near the upper slope, currents are northerly but weak, with small net transports of less than 0.2 Sv. Beginning at about the 2500m isobath, at a distance of ca. 100 km, LSW transport is equatorward, reaching its maximum cumulative transport of 7.5 Sv. at a distance/depth of

200km/3700m. The Overflow/LDW layer has a maximum transport in deeper water, it reaches its maximum cumulative equatorward transport of 12.5 Sv. at a distance/depth of ca. 260km/4200m. Because of the different phasing of the two layers, the sum of the two reaches its maximum cumulative transport of –19 Sv., midway between the above two locations.

The deep flow of the Gulf Stream, which we have only sampled on two cruises, eventually overcomes the equatorward transport in the DWBC. The outer boundary of our section is not the point beyond which there is no deep flow. So it would be incorrect to assume that the accumulated transports shown are net transports across a section between Cape Cod and Bermuda. Our focus with the present data set is with the deep equatorward flow along the steep bathymetry of the continental slope. The DWBC we find there is well-defined by the present data set, but we can say little here about offshore recirculation, except to note that it occurs, as can be readily seen with the poleward transport of LSW and Overflow/LDW in the Gulf Stream.

We have also calculated the transport of the upper layer and for the whole water column, a cumulative transport of -18 Sv at 200km and +84Sv at the offshore edge. The net transport of the Gulf Stream would be the difference of these two numbers (102 Sv) if our outer boundary were across all of the Gulf Stream. While our total transport figure is intermediate between those at 73W (93.7 Sv.) and 68W (112.8 Sv.) according to Johns *et al*. (1995), it is most probably underestimated.

4. **Effect of Warm-Core Rings on DWBC**

Our ensemble mean property section did not include data from one of the cruises: EN311. During this cruise, a Warm-Core Ring (WCR) is located along the station line (Figure 5). Substantial flow anomalies are present throughout the water column. Upper ocean flows are anticyclonic and generally follow what one would infer from the sea surface temperature imagery (e.g., Joyce, 1984). Deep flows are in the opposite direction from

the long-term ensemble means previously shown. It is clear from this one example that WCRs are capable of disrupting the flow in the DWBC. In another example (Amy Bower, personal comm., 2004), deep (3000m) floats have been observed to be displaced within the DWBC by a WCR and in some cases completely leave the deep flow along the continental slope. Our EN311 section did not go offshore far enough to determine if the DWBC flow was completely blocked or merely diverted around the southern periphery of the ring. In the latter case the WCR would not alter DWBC transports, only where they are found. With these problematic EN311 stations, amounting to about 10% of our total stations, one might be able to better gauge the overall effect of WCRs on DWBC transport if we also knew how often a WCR was over the section and how typical were our EN311 flow observations. On the former point, we can make use of the Brown et al. (1986) estimates of WCR probability density structure for a swath 50 km wide (roughly one ring radius) along the line of our section of length 200 km in the Slope Water. We estimate a probability of 0.2 that on any given day a WCR will be found within this area. This is quite high, higher than the percentage of stations made when a WCR was present, and suggests that the following lower DWBC transport estimate may be closer to the truth than our upper. However, without a better knowledge of the circulation anomalies caused by WCRs, we have little confidence that our single realization can be regarded as 'typical'. If EN311 is merely included as if it were like all of the other cruises, one can see its effect on transport to gauge what might be the range of uncertainty of DWBC transport (Fig. 6). The range in the total deep transport (black lines) amounts to –19 Sv (w/o the WCR) to –14 Sv with the WCR. For simplicity, we estimate the transport of the DWBC to be –16.5 ±2.5 Sv., with the 'error' associated with effects due to WCRs. This uncertaintity is comparable to what we estimate could arise due to other variability, such as TRWs.

5. **Discussion**

The transport numbers for our section are close to those of Pickart and Smethie (1998), who estimate a DWBC transport of –18.9 Sv at 55^{o}W. Yet our transport structure is only weakly tied vertically and horizontally to structure of the water masses. Thus our result is

intermediate to Pickart and Smethie (1998) and Leaman and Harris. In the latter, tracer and velocity cores are not coincident. All three locations must address the issue of recirculation. Our section is at the extreme western edge of the northern recirculation gyre, and according to Hogg *et al*., this gyre is found in deeper water between the Gulf Stream and the continental slope. Yet clearly there is some recirculation occurring within and to the southeast of the Gulf Stream at our 70^{o}W section. Deep LSW and Overflow waters can be seen heading back to their northern sources within the deep Gulf Stream. Deep recirculation on the seaward side of the Gulf Stream is also a feature of the western N. Atlantic (Worthington, 1976). The pathway by which the DWBC crosses under the Gulf Stream (Pickart and Smethie, 1993) involves not only these deep recirculation gyres, but also time dependence, allowing tracers to cross 'mean' flows with a sufficiently large time-dependent velocity.

The equatorward-flowing waters are confined between water depths of 2500 and 4000m, and while there is some slight tilt to the isolines in the plane of the section and a slight increase in equatorward flow of the Overflow water, the flow in the DWBC at 70^{o}W is barotropic in nature, and thus largely invisible to normal hydrography. This illustrates the value of the direct velocity observations in defining the structure and amplitude of this flow. Inshore of the 2500m isobath, flow rates in the LSW layer decrease, while the tracer signature does not, in contrast to the observations further upstream at 55^{o}W, where LSW characteristics and flow are greatest on the boundary. Inshore of the 4000m isobath, the total, vertically-averaged equatorward transport is 25 Sv.

Our equatorward transport of NADW in the DWBC amounts to 16.5 ±2.5 Sv. To what extent is this the total cold water transport in the thermohaline circulation? Schmitz and McCartney (1993) estimate that about 16 Sv of LSW and Overflow/LDW are exported to the south from the subpolar gyre. While this would seem to fit well with our estimate, we note that 4 Sv of their flow is deep enough that it cannot pass between Bermuda and the continental slope, but must go around the eastern edge of the Bermuda Rise and rejoin the DWBC between our location and Abaco. Schott et al. (2004) estimate at 50^{o}W from hydrographic, LADCP, and moored current meter records, that approximately 13 Sv. of

NADW is exported from the subpolar gyre in the DWBC. [We use their upper potential density limit of σ_0=27.68 kg/m^3 , which is equivalent to our upper bound of γ_n=27.8 kg/m^3 using neutral density.] Their transport figure is lower than the Schmitz & McCartney estimate and less than that published by Pickart and Smethie at 55^{o}W. The situation at Abaco contrasts the large DWBC transport of Leaman and Harris with that of Lumpkin and Speer (2003), who estimate that 17.6 ±2.7 Sv of NADW is transported equatorward across 24^{o}N. In the latter, slightly different neutral density levels were used to identify NADW, and the best-constrained transport figure is for the section mean, not the DWBC itself. Because of the hydrographic sections used in their inverse model, they can provide no estimate closer to the latitude of our section for further comparison. Thus, it would appear that there is no previously published DWBC transport figure for our 70^{o}W section south of Cape Cod, but given the error bars in various estimates, our results at 70^{o}W are generally consistent with what is known for the western N. Atlantic.

Acknowledgements

We wish to acknowledge the support of NSF grant OCE-0241354, and velocity data provided from site "W" (J. Toole) and from the KN173 leg 2 (Martin Visbeck). This is WHOI contribution # xxxxx.

References

Brown, O. B., P. C. Cornillon, S. R. Emmerson, and H. M. Carle, 1986. Gulf Stream warm rings: a statistical study of their behavior, *Deep-Sea Res*., 33, 1459-1474.

Doherty, K. W., D. E. Frye, S. P. Liberatore, and J. M. Toole, 1999. A moored profiling instrument. *J. Atmos. and Oceanic. Tech*., 16, 1816-1829.

Fine, R., and R. L. Molinari, 1988. A continuous deep western boundary current between Abaco (26.5^{o}N) and Barbados (13^{o}N). *Deep-Sea Res*., 35, 1441-1450.

Fischer, J., and M. Visbeck, 1993. Deep profiling with self-contained ADCPs, *J. Atmos. Oceanic Tech*., 10, 764-773.

Hogg, N. G., R. S. Pickart, R. M. Hendry, and W. J. Smethie Jr., 1986. The Northern Recirculation Gyre of the Gulf Stream, *Deep-Sea Res*., 33, 1139-1165.

Johns, W. E., T. J. Shay, J. M. Bane, and D. R. Watts, 1995. Gulf Stream structure, transport, and recirculation near 68^{o}W, *J. Geophys. Res*., 100, 817-838.

Joyce, T. M., 1984. Velocity and Hydrographic Structure of a Gulf Stream Warm-Core Ring, *J. Phys Oceanogr*., 14, 936-947.

Leaman, K. D., J. E. Harris, 1990. On the Average Absolute Transport of the Deep Western Boundary Currents East of Abaco Island, the Bahamas *J. Phys. Oceanog*. 20, 467-475.

Lumpkin, R. and K.Speer, 2003. Large-Scale Vertical and Horizontal Circulation in the North Atlantic Ocean, *J. Phys. Oceanogr*., 33, 1902-1920.

Pickart, R. S., and W. M. Smethie Jr., 1998. Temporal evolution of the deep western boundary current where it enters the sub-tropical domain. *Deep-Sea Res*. I, 45, 1053-1083.

Pickart, R. S., and W. M. Smethie Jr., 1993. How does the Deep Western Boundary Current cross the Gulf Stream? *J. Phys. Oceanog*., 23, 2602-2616.

Schmitz, W. J., Jr., and M. S. McCartney, 1993. On the North Atlantic Circulation, *Rev. Geophys*., 31, 29-49.

Schott, F. R., R. Zantopp, L. Stramma, M. Dengler, J. Fischer, and M. Wibaux, 2004. Circulation and Deep-Water Export at the Western Exit of the Subpolar North Atlantic, *J. Phys. Oceanogr.,* 34, 817-843.

Worthington, L. V., 1976. On the North Atlantic Circulation, *The Johns Hopkins Oceeanogr. Stud.*, 6, 110pp.

Tables

Table 1. Summary of cruises providing data

Line W Cruise Table		
Cruise	**Date**	**Comment**
en257	Nov-94	10 stas., BOUNCE
oc269	Jun-95	4 stas., 3 w/LADCP, BOUNCE
en283	May-96	7 stas., PRIMER
en286	Aug-96	8 stas., PRIMER
en295	Feb-97	5 stas., PRIMER
en311	Dec-97	6 stas., WCR present, PRIMER
oc371	Oct-01	4 stas., deploy "W" mooring
station W	Sep-02	end of 1 year-long average at "W"
kn173_2	Oct-03	17 stas., Repeat Hydro.

Table 2. Neutral Density Layers used to define volume transport

Layer #	Neutral Density Range (kg/m^3)	Comment
1	25.000: 27.800	Upper Water
2	27.800: 27.975	Upper and Classical LSW
3	27.975: 28.140	Overflow, LDW

Figure Captions

Figure 1. Bathymetric contours (contour interval 500m) showing collection of stations used in defining a mean cross section. The circle symbol at the inshore edge is taken to be the 'origin' of our coordinate system. It is located at a depth of 210m at the shelf break.

Figure 2. Mean property sections from the CTD data shown relative to a shelf break origin and along a line defined by the aggregate of the stations (Fig. 1). Potential Temperature (left), Salinity (center) and Dissolved Oxygen (right). Solid lines and colors represent each of the different variables plotted, while dashed lines are neutral density surfaces (see Fig. 3, center).

Figure 3. Planetary Potential Vorticity (left) is plotted on a scale that illustrates the low PV values in LSW and the sharp gradient of PV found between the Overflow Waters and the underlying LDW. Neutral Density (center) and Normal Velocity (right) are also given. For the latter, the thick dashed contour is for zero velocity and positive values are poleward.

Figure 4. Layer-averaged transport (left panel) and cumulative transport (right panels) in neutral density layers encompassing LSW (solid lines and x's), Overflow and LDW (dashed lines and circles), and their sum (dotted lines and pluses). Cummulative transport (in Sv, $=10^6$ m^3/s) is initialized at the shelf break and plotted against offshore distance (left two panels) and water depth (right panel).

Figure 5. SST image (from the Johns Hopkins Univ. Applied Physics Laboratory website) showing a composite SST image for 1-7 December 1997 and hydrographic stations taken during EN311 from 2-4 December. Magenta vectors are from LADCP data averaged in the upper 200m and blue vectors are averages between 1500m depth and the local bottom.

Figure 6. Deep Layer-averaged transports (as in Fig. 4) with and without the EN311 section, which includes a WCR. Generally, the presence of the WCR reduced deep southward transports and this defines the low transport branch in the two panels, which show transport in 20 km-wide portions of the section (left) and accumulated transport (right).

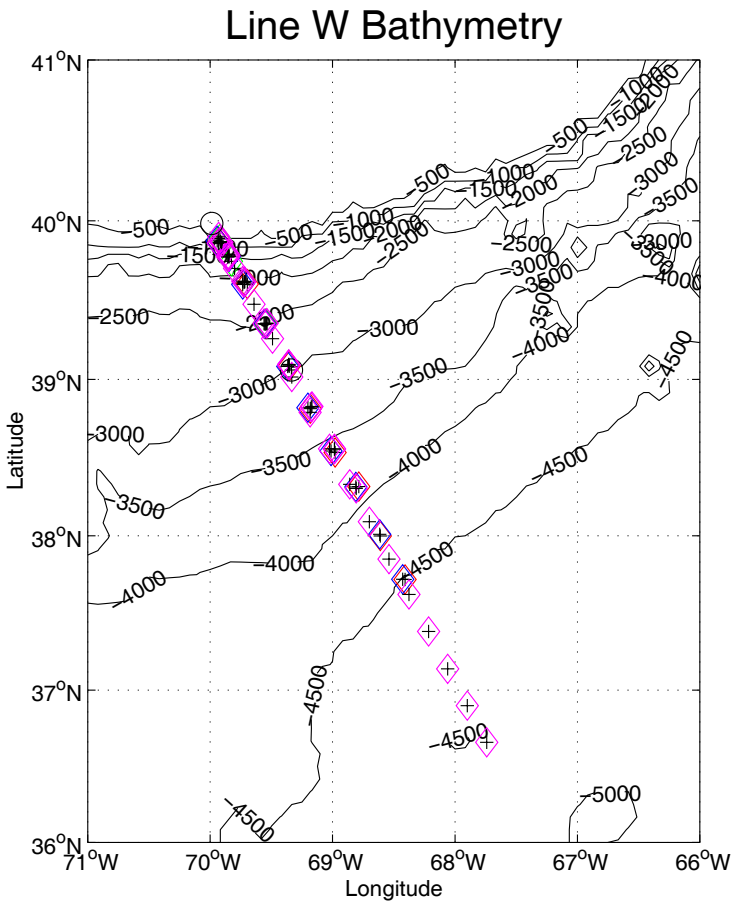
Line W Bathymetry
41°N
40°N
39°N
38°N
37°N
36°N
71°W
70°W
69°W
68°W
67°W
66°W
Latitude
Longitude
500
1000
1500
2000
2500
3000
3500
4000
4500
5000

Figure 1

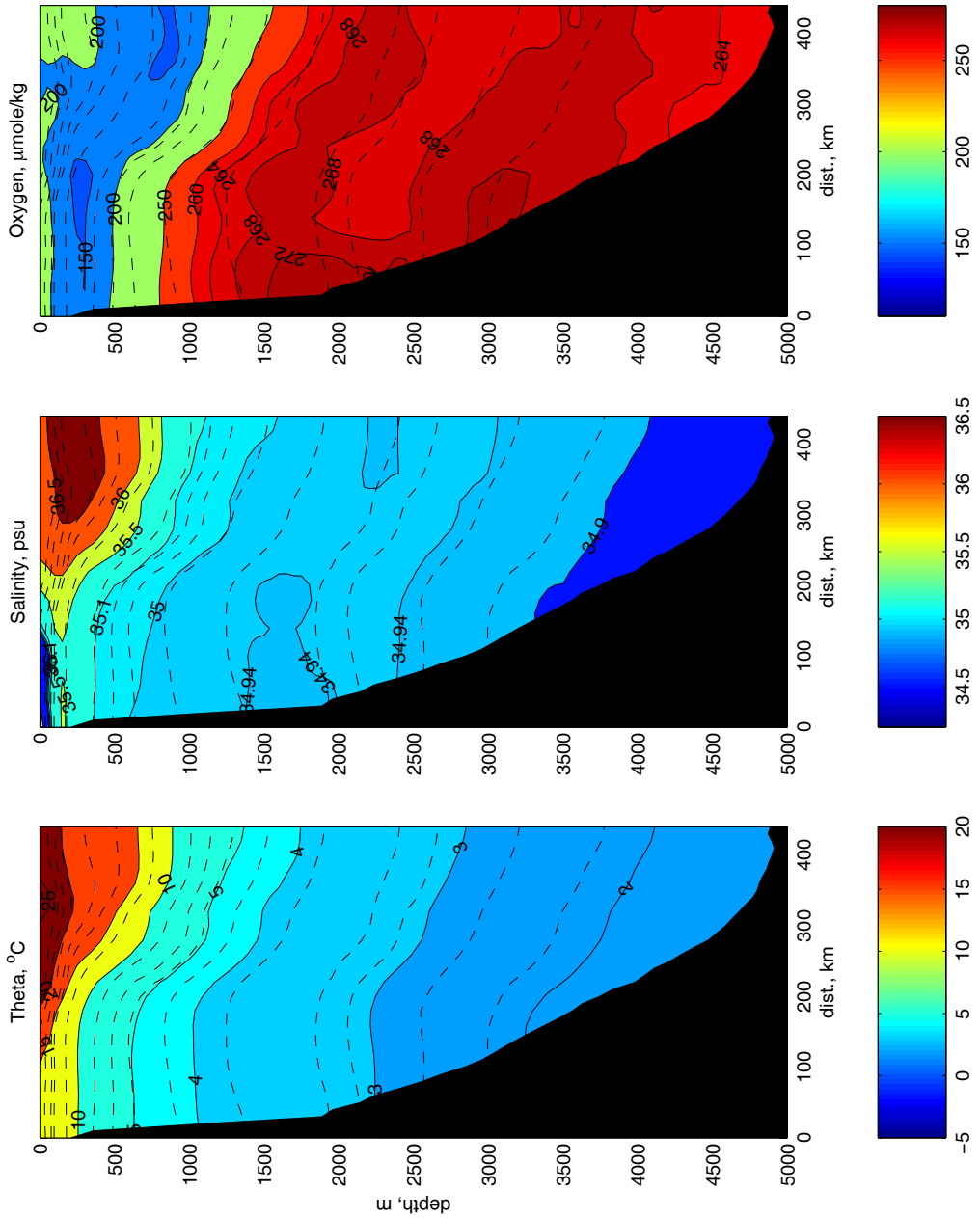

Figure 2

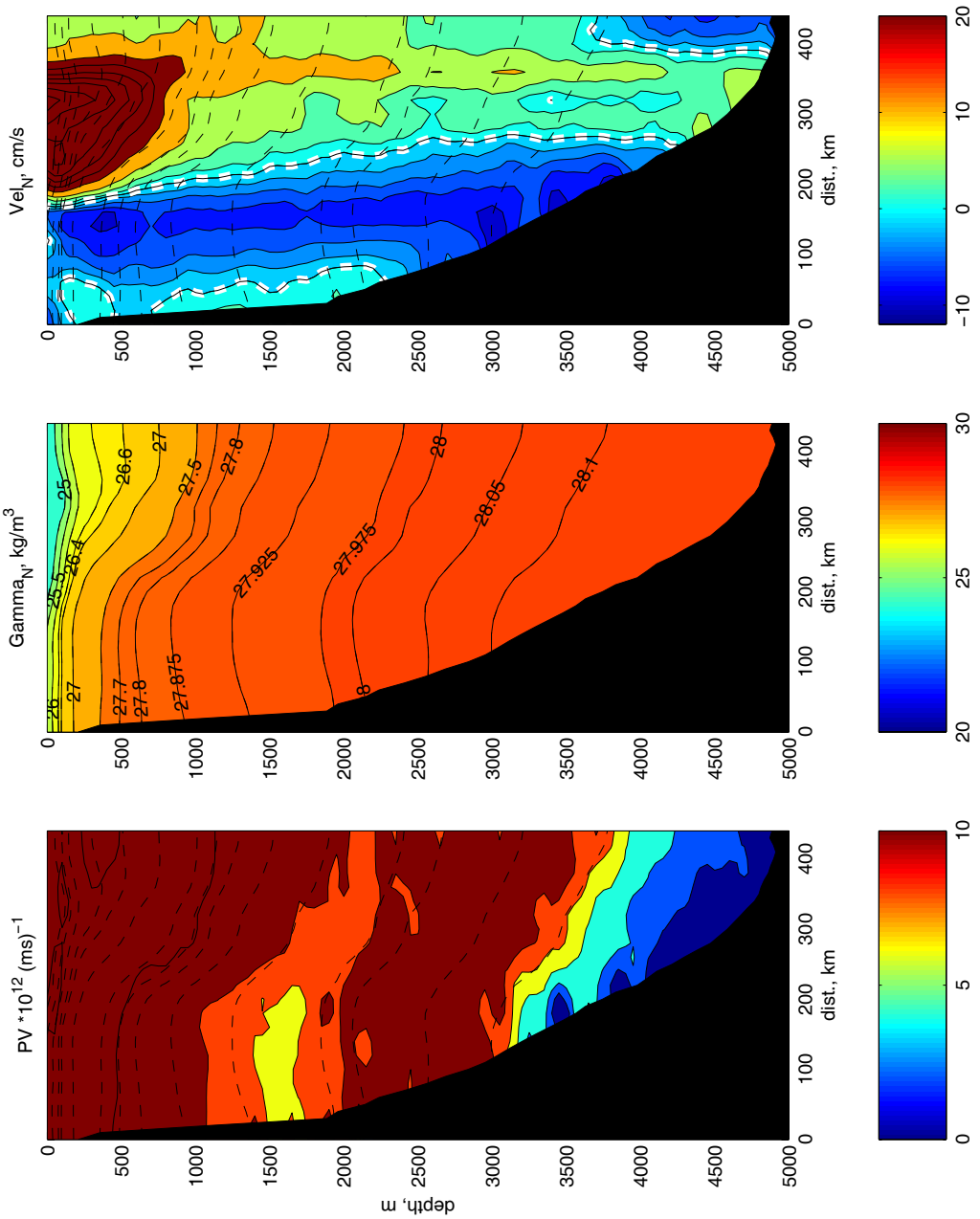
Vel$_N$, cm/s
Gamma$_N$, kg/m^3
PV *10^{12} (ms)$^{-1}$
depth, m
dist., km
0
500
1000
1500
2000
2500
3000
3500
4000
4500
5000
100
200
300
400
−10
0
10
20
25
30
5
26
26.4
26.6
27
27.5
27.8
27.925
27.975
28
28.05
28.1
27.7
27.875

Figure 3

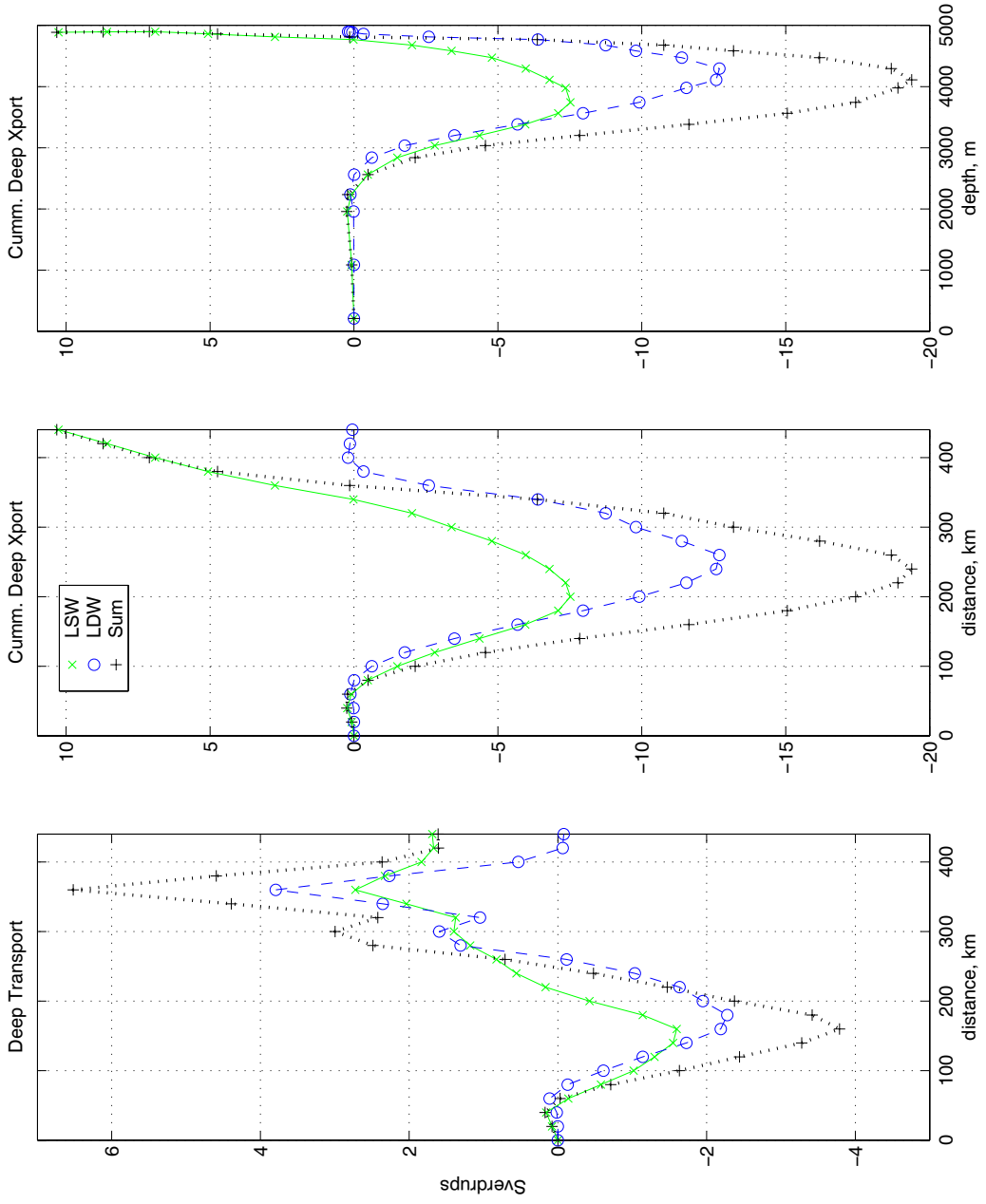
Cumm. Deep Xport
depth, m
Cumm. Deep Xport
LSW
LDW
Sum
distance, km
Deep Transport
distance, km
Sverdrups

Figure 4

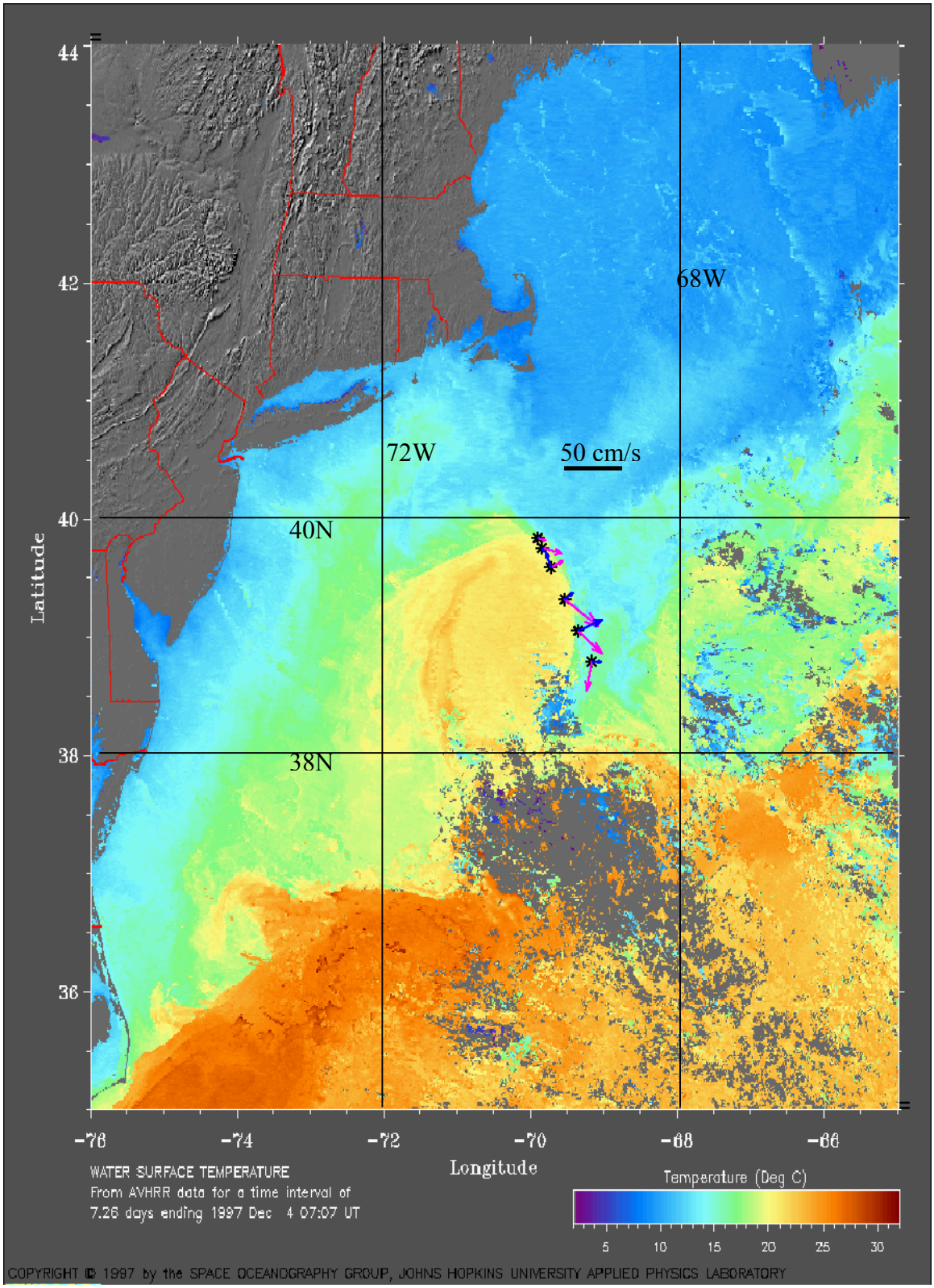
44
42
40
38
36
Latitude
68W
72W
50 cm/s
40N
38N
-76
-74
-72
-70
-68
-66
Longitude
WATER SURFACE TEMPERATURE
From AVHRR data for a time interval of
7.26 days ending 1997 Dec 4 07:07 UT
Temperature (Deg C)
5
10
15
20
25
30
COPYRIGHT © 1997 by the SPACE OCEANOGRAPHY GROUP, JOHNS HOPKINS UNIVERSITY APPLIED PHYSICS LABORATORY

Figure 5

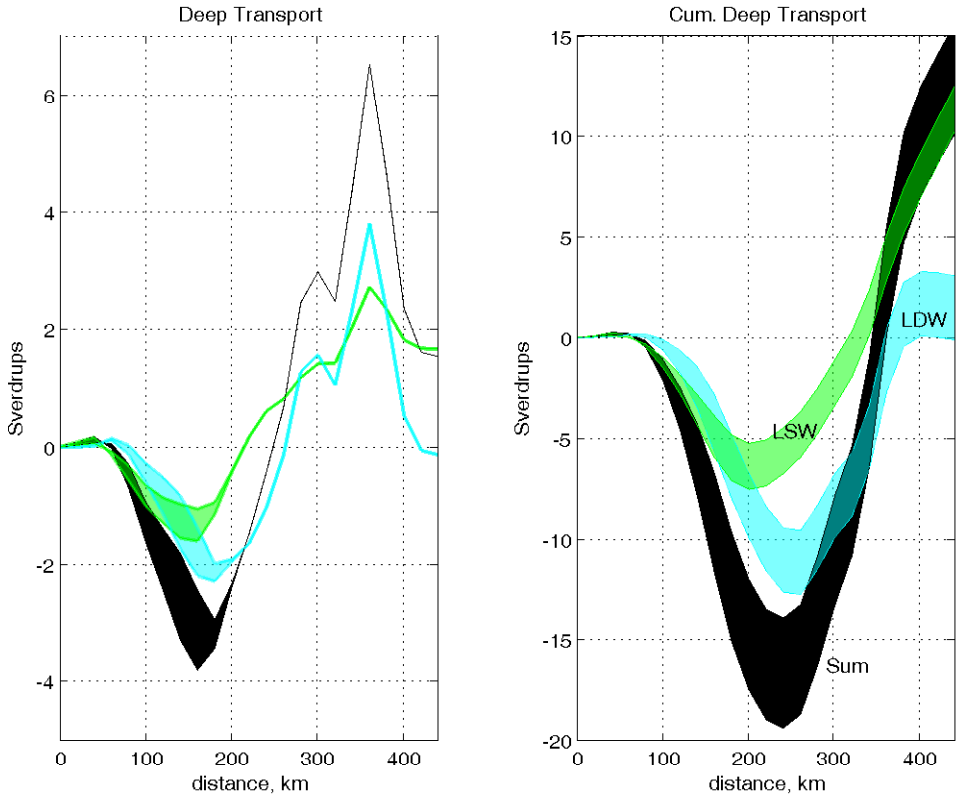
Deep Transport
Sverdrups
distance, km
Cum. Deep Transport
Sverdrups
distance, km
LDW
LSW
Sum

Figure 6